

Supplementary Material

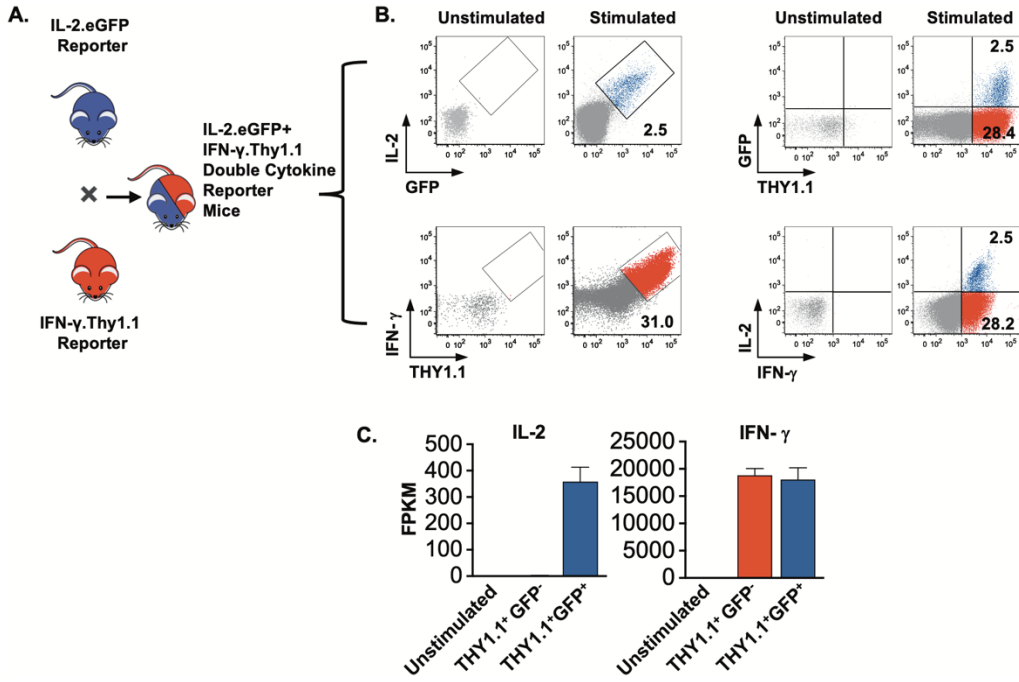


Figure S1. Generation and authentication of IFN- γ .Thy1.1 IL-2.GFP double cytokine reporter mice.

(A) Schematic of the generation of IFN- γ .Thy1.1 IL-2.GFP double cytokine reporter mice. IL-2.GFP and IFN- γ .Thy1.1 reporter mice were intercrossed and then further bred to generate homozygous IFN- γ .Thy1.1 IL-2.GFP double cytokine reporter mice.

(B) The correlation between IL-2 and GFP expression (top) and IFN- γ and Thy1.1 (bottom) was tested using a two color cytokine secretion assay (Miltenyi) using splenic effector CD8 T cells at 9 days following LCMV-ARM infection. Cells were either left untreated or stimulated with a cocktail of GP33, GP276, and NP396 peptide epitopes (1 μ g/mL each) for 3.5hr followed by a 45min period of secretion assessment with the catch reagents.

(C) FPKM values of *iL2* and *ifng* derived from RNA-seq analysis of sorted unstimulated, and LCMV-GP33 stimulated P14-specific GFP+THY1.1+ and GFP-THY1.1+ effector CD8 T cells procured at 9 days post infection.

Figure S2

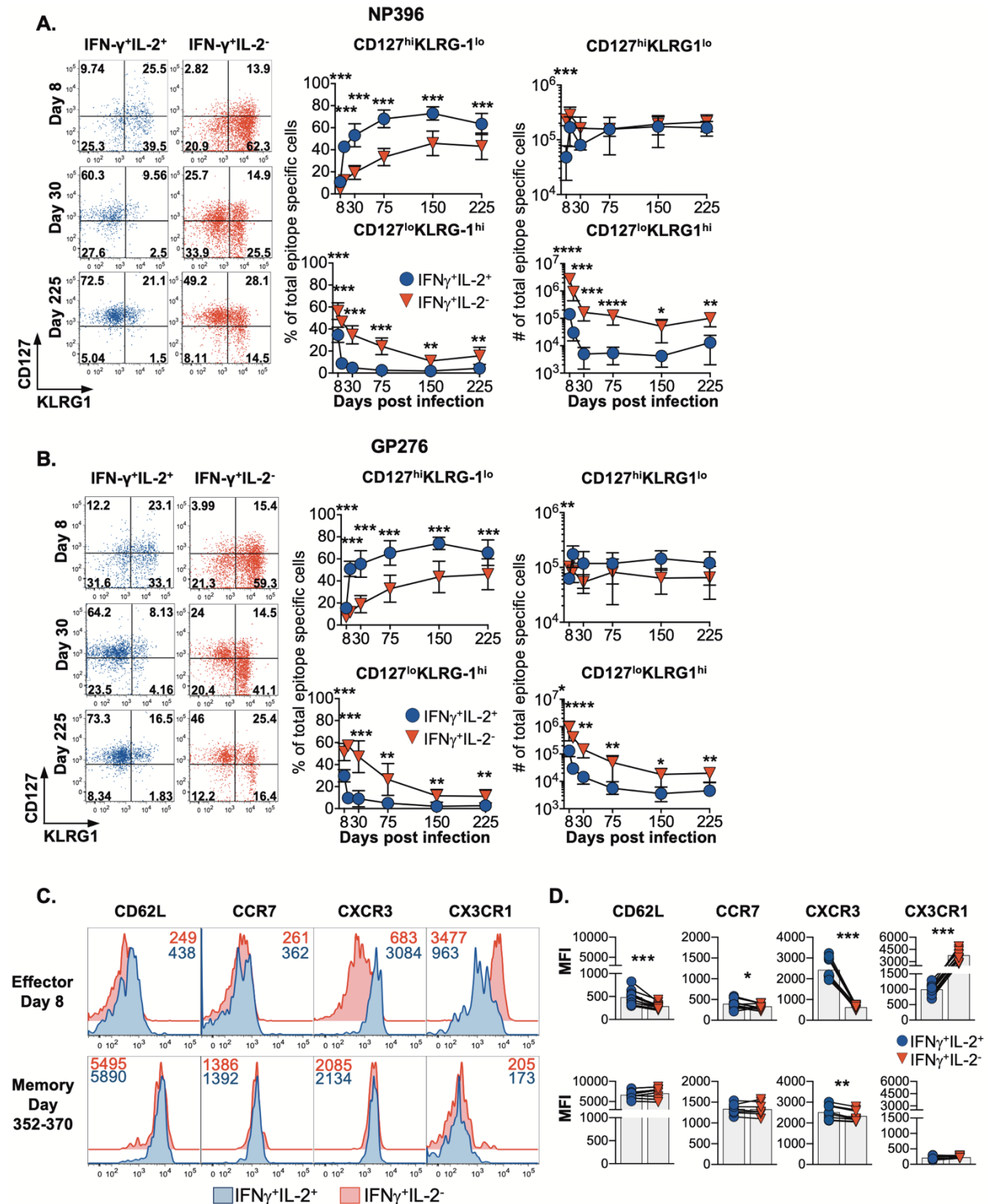


Figure S2. IL-2-producing effector CD8 T cells more rapidly attain a canonical memory phenotype.

Analysis of CD127 and KLRG1 expression by splenic IL-2-producing (IFN- γ ⁺IL-2⁺; blue) and non-IL-2-producing (IFN- γ ⁺IL-2⁻; red) LCMV NP396 epitope-specific (A) and LCMV GP276-specific (B) CD8 T cells over time following acute LCMV infection. (C-D) The expression of select effector- and memory-associated molecules by IL-2 producing (blue) and non-producing (red) LCMV-specific P14 CD8 T cells at effector and memory time points following adoptive transfer and priming by acute LCMV infection. Composite data are shown from 3 experiments analyzing a total of 6-12 mice per group. p values were calculated using paired two-tailed t tests.

*p<0.05, **p<0.01, ***p<0.001

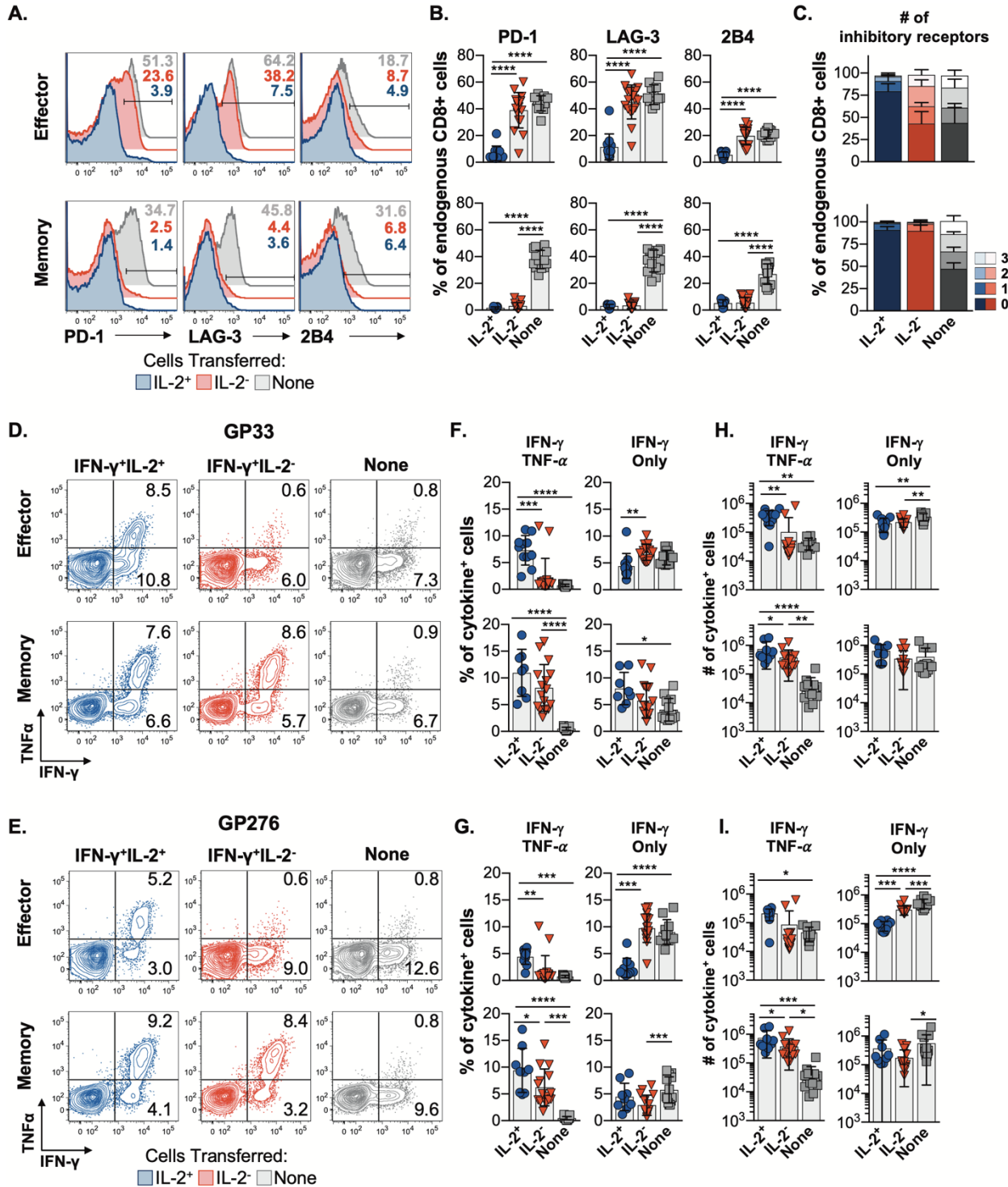


Figure S3. IL-2⁺ effector as well as IL-2⁺ and IL-2⁻ memory CD8 T cells rescue the endogenous response following chronic viral challenge.

(A) Representative flow histograms and (B) composite data showing the expression of PD-1, LAG-3, and 2B4 by the recipients' endogenous CD8 T cells recovered from mice that received donor NP396-specific IFN- γ ⁺IL-2⁺ (blue) or IFN- γ ⁺IL-2⁻ (red) effector (top) or memory (bottom) CD8 T cells and were then challenged with LCMV-clone 13 as in Figure 3A. Responses in control mice that did not receive donor cells (none; gray) are also shown.

(C) The percentage of endogenous CD8 T cells which co-express 0, 1, 2, or 3 inhibitory receptors.

(D-E) Flow cytometry plots, (F, G) percentages and (H, I) numbers of IFN- γ and TNF- α producing LCMV GP33- (D, F, H) or GP276- (E, G, I) specific endogenous CD8 T cells from recipients that received IFN- γ ⁺IL-2⁺ (blue) or IFN- γ ⁺IL-2⁻ (red) effector (top) or memory (bottom) CD8 T cells, or that did not receive donor cells (gray).

Representative or composite findings are shown from 3 experiments analyzing a total of 9-16 mice per group. Bar graphs show mean \pm SD with p values calculated using one-way ANOVA.

*p<0.05, **p<0.01, ***p<0.001, ****p<0.0001

Figure S4

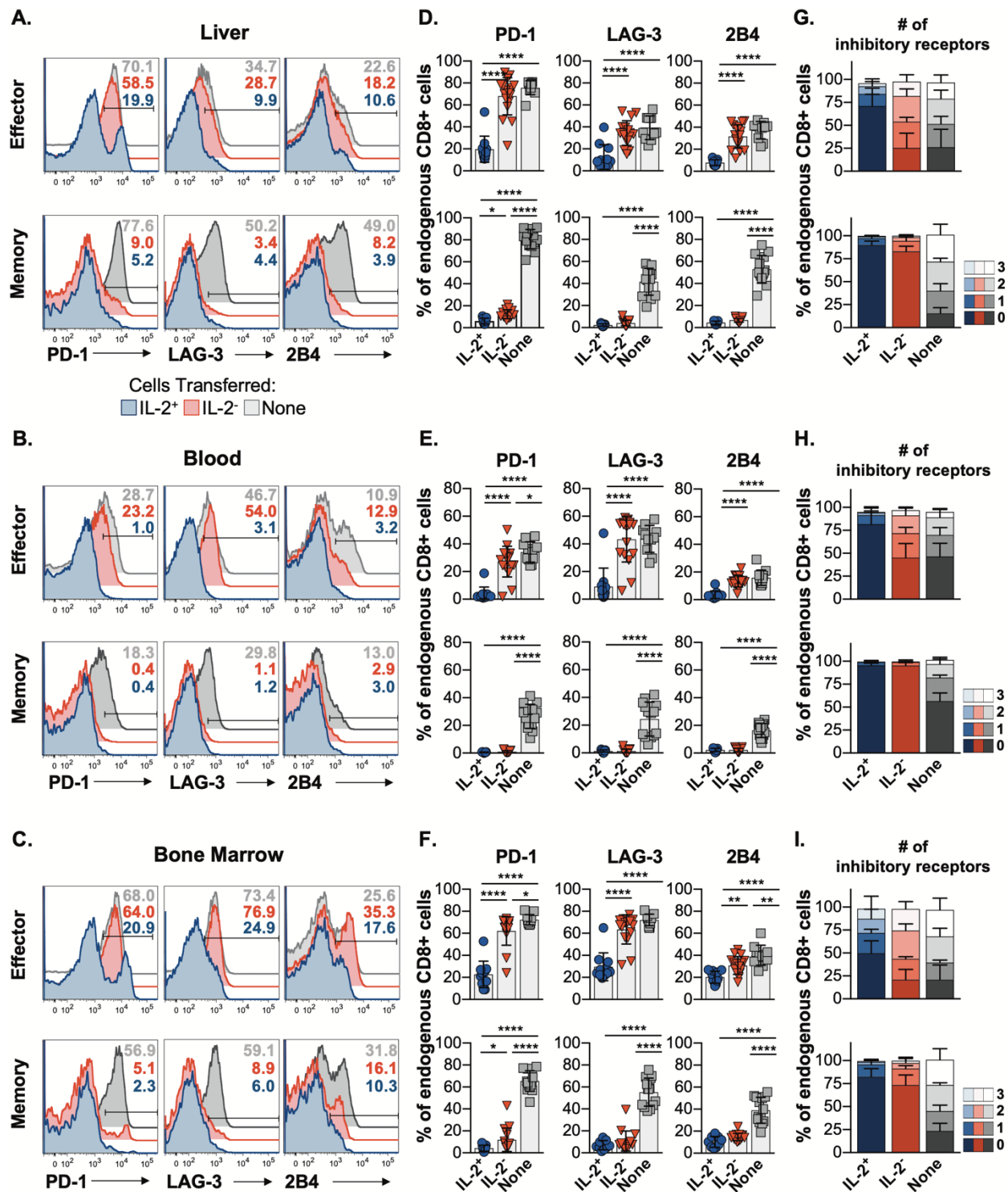


Figure S4. Endogenous CD8 T cells become exhausted in the presence of non-IL-2-producing effector cells.

(A-C) The expression of PD-1, LAG-3, and 2B4 by the recipients' endogenous CD8 T cells recovered from the liver (A), blood (B), and bone marrow (C) of mice that received donor NP396-specific IFN- γ ⁺IL-2⁺ (blue) or IFN- γ ⁺IL-2⁻ (red) effector (top) or memory (bottom) cells.

Responses in control mice that did not receive donor cells (none; gray) are also shown. Cell transfers, LCMV-clone 13 challenge, and analyses were conducted as depicted in Figure 3A.

(D-F) Composite data of PD-1, LAG-3, and 2B4 expression by endogenous CD8 T cells recovered from the liver (D), blood (E), and bone marrow (F) of the indicated cohorts of recipients at 14 days post-challenge.

(G-I) Bar graphs depict the proportion of endogenous CD8 T cells recovered from the liver (G), blood (H), and bone marrow (I) of the indicated cohorts of recipients that co-express 0, 1, 2, or 3 of the analyzed inhibitory receptors.

Representative or composite findings are shown from 3 experiments analyzing a total of 9-16 mice per group. Bar graphs show mean \pm SD with p values calculated using one-way ANOVA.

*p<0.05, **p<0.01, ***p<0.001, ****p<0.0001

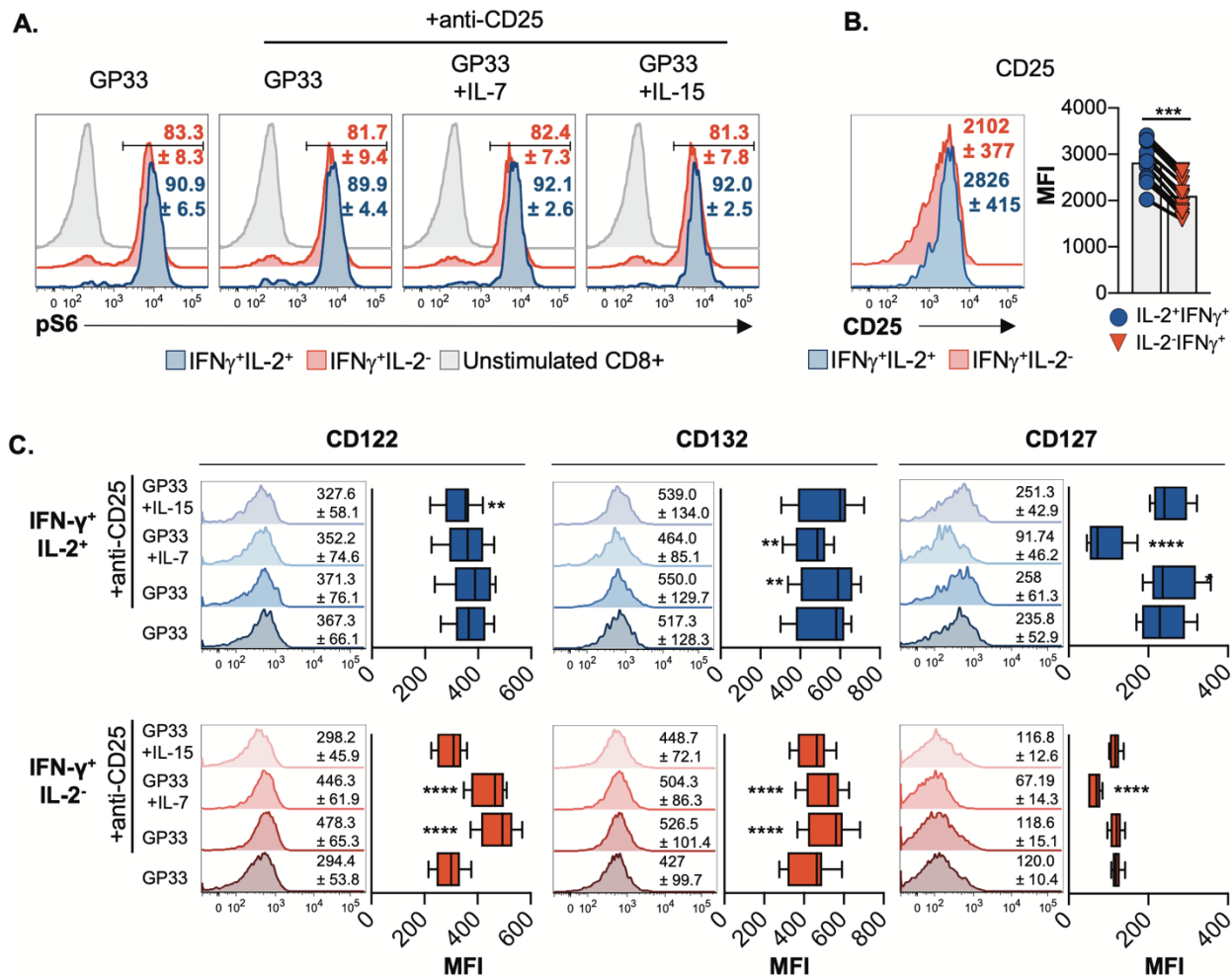


Figure S5. IL-2-producing and non-producing effector CD8 T cells are differentially sensitive to IL-2, IL-7, and IL-15.

(A) Splenocytes from LCMV-infected mice were prepared at eight days following LCMV infection and stimulated with a mix of GP33, NP396, and GP276 peptide epitopes in the presence or absence of anti-CD25 blocking antibodies for 5 hours. Certain samples were stimulated with recombinant IL-7 or IL-15 for the final 30 minutes of the culture period. Representative flow cytometry histograms show phosphorylated S6 (pS6) levels by IL-2-producing (IFN- γ ⁺IL-2⁺; blue) and non-producing (IFN- γ ⁺IL-2⁻; red) CD8 T cells. pS6 levels in unstimulated control cells are shown in gray. Numerical values given on the plots are percentages \pm SD. (B) Representative flow histograms (left) and composite results (right) show

CD25 expression by IL-2-producing and non-producing P14 LCMV-specific CD8 T cells at 8 days post infection, following stimulation with the GP33 peptide. (C) The CD122, CD132, and CD127 levels on IL-2 producing and non-producing P14 CD8 T cells procured and stimulated as described above. In (B) and (C) numerical values given on the plots are MFI \pm SD. p values were calculated using paired two-tailed t-test (B) and one-way ANOVA (C). Representative or composite results are presented from 3 independent experiments analyzing a total of 8-12 mice in each group. *p<0.05, **p<0.01, ***p<0.001, ****p<0.0001

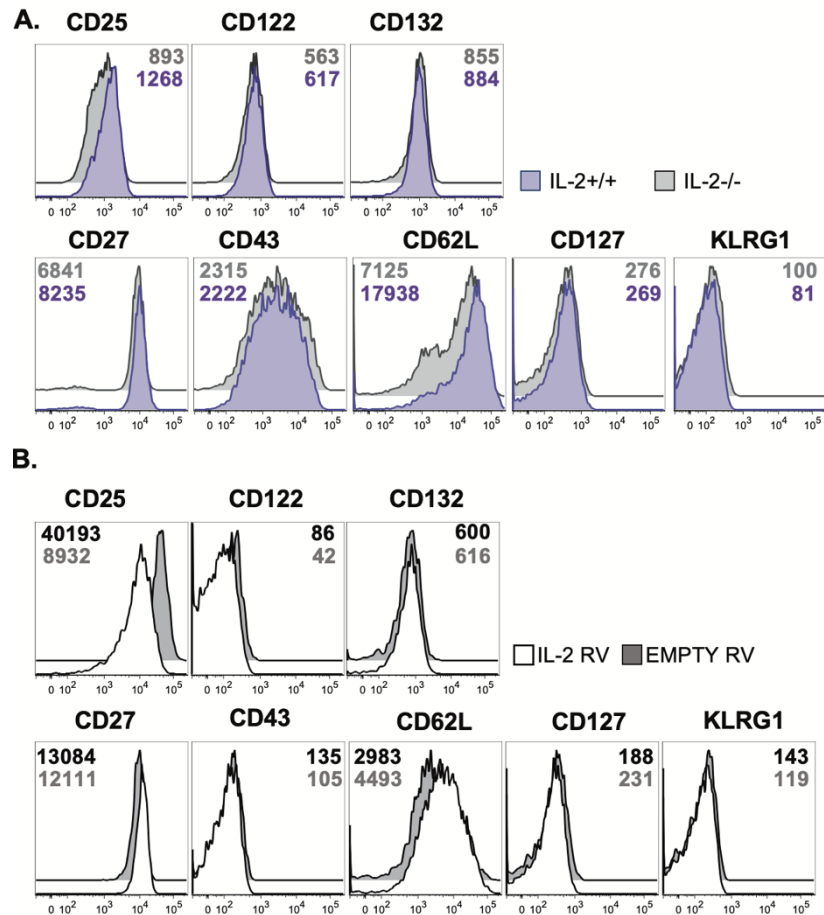


Figure S6. Phenotypic similarities of in vitro differentiated CD8 T cells.

(A) Purified naïve IL-2^{+/+} and IL-2^{-/-} P14 CD8 T cells were stimulated with GP33 peptide pulsed irradiated feeder cells and cultured using a staggered IL-2 and IL-15 regime for a total of 5 days prior to assessing phenotypes.

(B) Purified naïve splenic P14 CD8 T cells were activated with anti-CD3 and anti-CD28 antibodies and retrovirally transduced with either empty/ control or IL-2-expressing MSCV. The phenotypes of the transduced GFP-expressing cells were then assessed.

In each case representative data from one of 3 experiments are shown.

Figure S7

GATING STRATEGIES

Figure 1A-E, S2 A-B

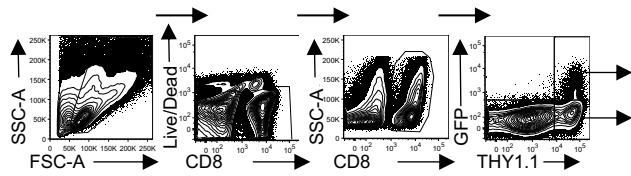


Figure 1F-G

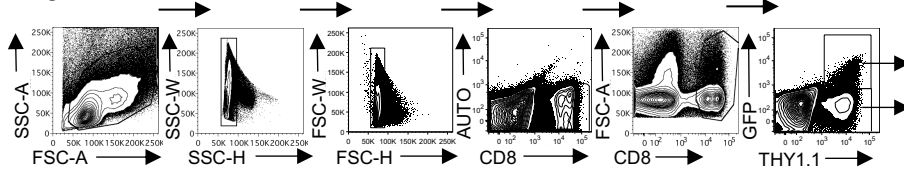


Figure 1H-I

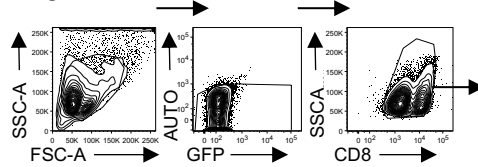


Figure 2A, 3A Sort

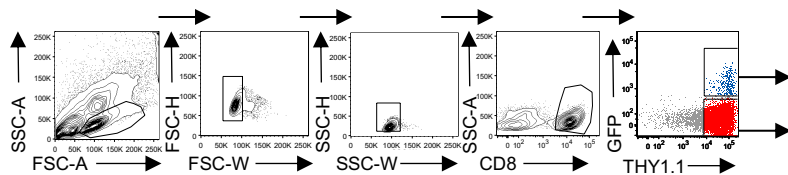


Figure 2B-E, S2C

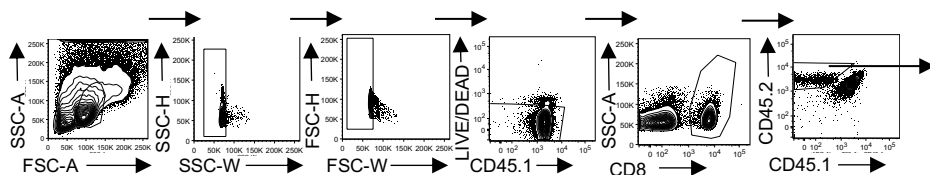


Figure 3B-C, 4A-H, S3, S4

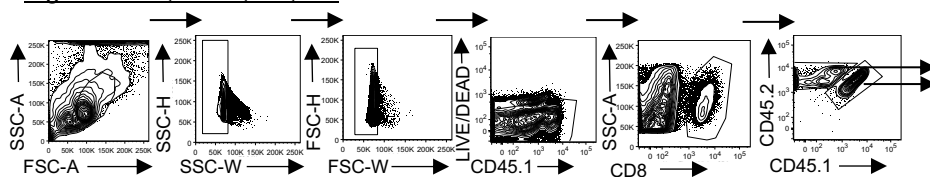


Figure 5 sort, S1C

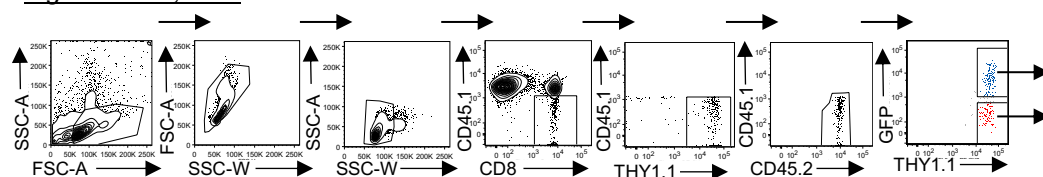


Figure S7 continued

Figure 6A

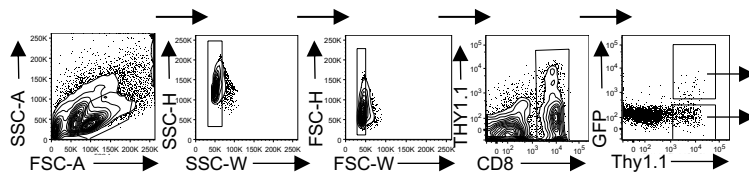


Figure 6B-C, S5A

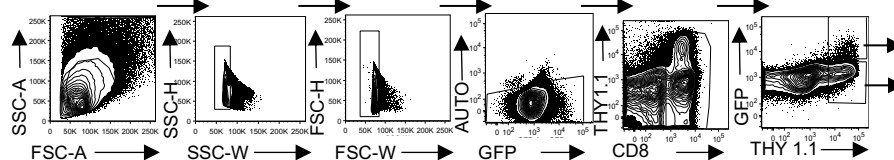


Figure 6D-E, S6

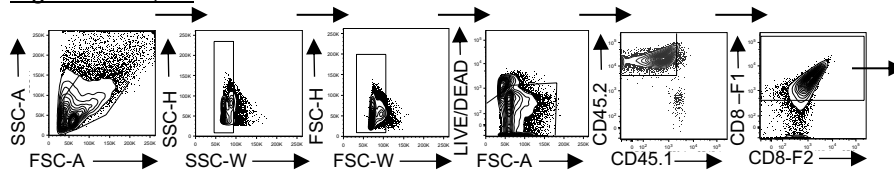


Figure 6F

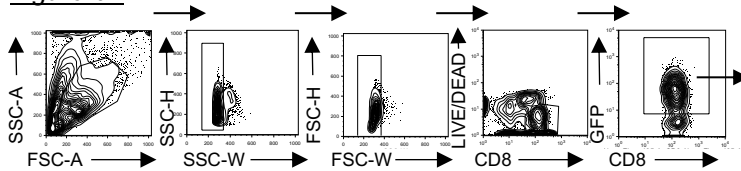


Figure 6G

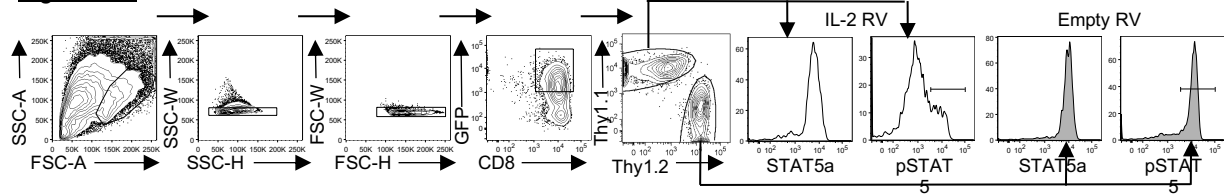


Figure S1B

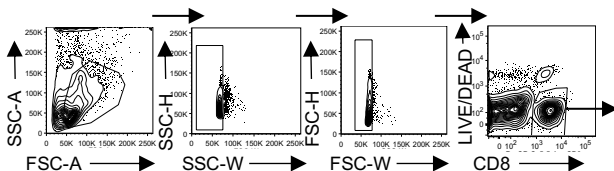


Figure S2C, S5B-C

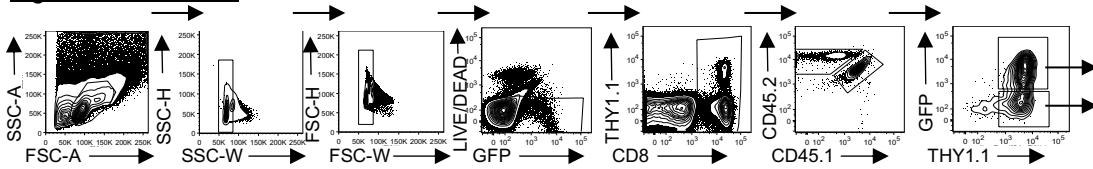


Figure S7. Flow cytometric gating strategies.

Each series of panels depict the flow cytometric gating strategies that were used in the indicated figures.